2021

Dynamic simulations of an absorption system with different working pairs at chiller and heat pump application

Jian Zheng
CTTC UPC, Spain

Jesús Castro

Carles Oliet
oliva@cttc.upc.edu

Dynamic simulations of an absorption system with different working pairs at chiller and heat pump application

J.Zheng[1], J.Castro[1*], C.Oliet[1]

[1] Heat and Mass Transfer Technological Center(CTTC), Universitat Politècnica de Catalunya-BarcelonaTech(UPC),
C/Colom,11,Terrassa,E-08222,Spain
+ 34 93 739 81 92,cttc@cttc.upc.edu

* Corresponding Author

ABSTRACT

This work describes the dynamic simulation of a direct air-cooled single effect solar-driven absorption system and demonstrates the numerical results of the absorption system with different working pairs. The working pairs used in the chiller mode are LiBr-H_2O and Carrol-H_2O (Carrol contains LiBr and EG -Ethylene glycol- with a mass ratio at 4.5:1), while in the heat pump mode, EG is introduced in the evaporator to avoid freezing problem which limits the operation condition. The numerical modelling was implemented on a modular object-oriented simulation platform (NEST platform tool), which allows the linking between different components, considered as objects, which can be either an empirical-based model or a more detailed CFD calculation if necessary. Specifically, flat plate collectors coupled with a storage tank is introduced assisting the heat source for the absorption system, and all the components are implemented based on mass, momentum, and energy balances. The goal of this work is to compare the general performance like *COP* and working capacity between LiBr-H_2O and Carrol-H_2O in chiller mode and the performance of working pair Carrol-H_2O at heat pump mode in dynamic operation. Finally, various simulations at each case are performed with meteorologic data of Barcelona and Madrid in summer and winter, and the heat source consists of 30 m^2 solar collectors and an auxiliary heater. The solar collectors used in the system are high efficiency flat solar collectors. The fraction of solar energy in heat source varies depends on the total radiation in the area, which could reach 0.65 on a sunny day or attributes less than 0.1 on a cloudy day.

1. INTRODUCTION

In the last years, the absorption system in climatization applications have driven more interest due to the policy of CO_2 emission reduction. For a domestic case, small capacity(less than 30kW) absorption systems could play an important role in the building climatization system. LiBr-H_2O is one of the most widely used working pairs for absorption system and the refrigerant water grants the eco-friendly advantage, besides, the heat source of the system could be solar-heated water, geothermal water, waste heat, or other low-grade heat. However, the working pair LiBr-H_2O could encounter the crystallization problem in the absorber and freezing problem in the evaporator while used as an air-sourced heat pump. These problems may interfere with the performance of the machine or cause damage to the apparatus. Thus, another working pair Carrol-H_2O proposed by R. Reimann (1979) is introduced to reduce the crystallization risk, while in the heating application, EG is introduced to the evaporator to avoid freezing problem.

For the absorption system in chiller or heat pump mode, many authors have studied with experiments or numerical models. Joudi & Lafta (2001); Florides et al. (2003) developed steady-state numerical models to predict the performance of an absorption refrigeration system using LiBr-H_2O as a working pair. Fu et al. (2006) developed a library of elemental dynamic models for absorption refrigeration systems with different working mediums and cycle configurations, which grants the library flexibility and extensibility. While steady-state modelling is widely applied to design or analysis the absorption systems, on the other hand, dynamic simulations also drove attention to predict the performance in a more complicate and realistic test campaign procedure. Zinet et al. (2012) explores the dynamic response of the system to basic input parameters change , and Iranmanesh & Mehrabian (2013) created a new algorithm for calculating the flow rate in a solution circulation, and validated the simulation results against a double-effect absorption chiller from startup to shutdown. Xu et al. (2016) investigated the effects of thermal mass and compared two different control strategies. Evola et al. (2013) proposed a model for the dynamic simulation of a solar-assisted single-stage LiBr-H_2O absorption chiller and validate the numerical model with a commercial absorption machine. Farnós et al. (2017) did

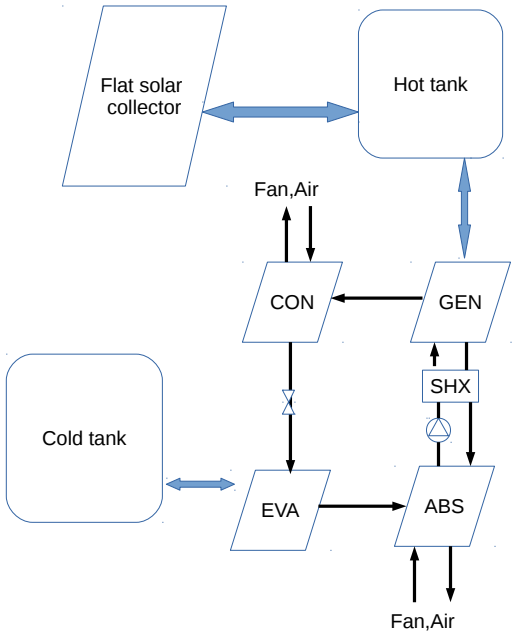

Figure 1: System of absorption system in different working conditions

dynamic modeling of an air-cooled LiBr-H_2O absorption chiller based on mass transfer empirical correlations.

Freezing phenomena at evaporator may also limit the application of the heat pump with absorption system using H_2O as a refrigerant. Many strategies have been used to overcome this issue. For heat pump application, reported in (Jeong et al. (1998); Koehler & Ibele (1988); Izquierdo & Aroca (1990); Cheng & Shih (1988); Lee & Sherif (2001); Şencan et al. (2005); Sun et al. (2010)), the evaporator was driven by solar-heated water,waste heat, or geothermal water, etc. On the other hand, Stepanov et al. (2015), present a study using LiBr as brine in the evaporator to achieve subzero temperatures.

Due to the crystallization and freezing risks, the direct air-cooled absorption system has not been developed much according to author's knowledge. In this work, a virtual machine combined with a absorption system and solar collectors are build to test the dynamic performance of the whole system with different working pairs. In previous work Castro et al. (2020), the transient model for the development of an air-cooled LiBr-H_2O absorption chiller based on heat and mass transfer empirical correlations was proposed. The numerical results were also compared with experimental data from Evola et al. (2013), shows a good agreement. The simulation of the machine under steady-state Q_{EVA} = 6kW and a *COP* of 0.74. The model was validated with experimental results with a small capacity (2-3kW) direct air-cooled machine in Castro et al. (2007). The aim of this work also includes the development of the laboratory prototype of an air-cooled absorption machine at heat pump mode. In this work, the dynamic model NEST is used for the simulation.

2. SYSTEM DESCRIPTION

2.1 Absorption system description

Figure 1 shows the system in this work, which consists of absorption system and hot/cold storage tank and flat solar collectors. The hot tank is connected with the generator, collector and integrated with an auxiliary heater, thus a differential control strategy is used here to maintain the generator secondary circuit temperature in range of 75-90°C. Figure 2 shows the two modes of absorption system: a) heat pump and b) absorption chiller. The absorption machine is air-cooled, with a vertical arrangement of the components, as shown in the picture. The air is drove by the fan and passes through the absorber and condenser. In the heat pump mode, the absorption machine works inside the building,

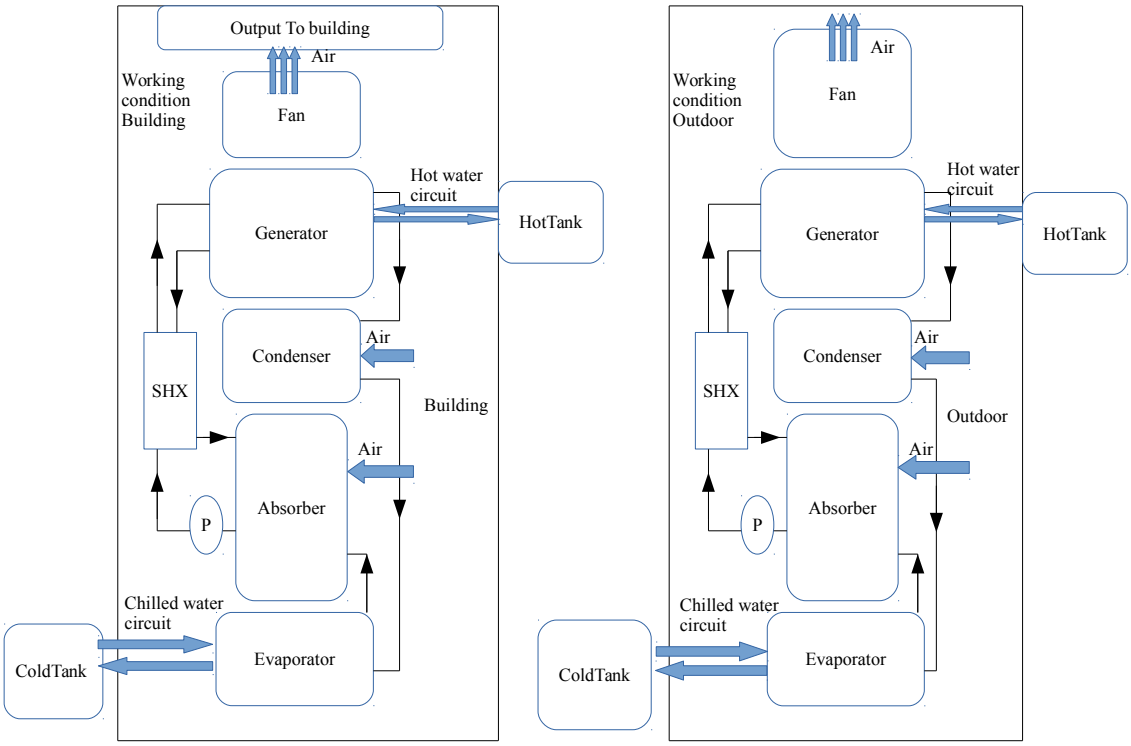

Figure 2: System of absorption system in different working conditions

the evaporator secondary circuit will take heat from the cold tank circuit, which is operated at ambient temperature, and there will be heat rejected from the absorber and condenser as output to heat the building. In the chiller mode, the ambient for the machine is the outside condition. In this case, the chilled water in the evaporator secondary circuit will be sent to the cold tank as cooling output. The ambient temperature is either set as a fixed value or be set as climatization data extracted from Barcelona or Madrid. The temperature inside the building is set to 20°C. The cold tank temperature is set as 14°C in the chiller mode and in the heat pump mode, the temperature of the cold tank is set to ambient temperature. Inside the absorption system, working pairs LiBr-H_2O and Carrol-H_2O are used in comparison in the chiller mode, while in the heat pump mode, EG is introduced to the evaporator to avoid freezing problem. The mass concentration of EG in the evaporator in heat pump mode is set to 10%, 30% according to the lowest temperature in Barcelona, Madrid, respectively.

2.2 Assumption for the theoretical cycle

The following assumptions have been made in the development of numerical modeling:
(i) The analysis is made under transient conditions.
(ii) The components are considered well insulated.
(iii) Pressure change in the components is considered negligible except valves and pumps.
(iv) Crystallization is not directly imposed in the simulation, the results are compared against the crystallization curve to assess the cycle.
(v) The vapor temperature is the same as the outlet temperature of the corresponding liquid.
(vi) The secondary cycle is operated under atmospheric conditions.
(vii) The solar collector is set to a fixed angle.

2.3 Numerical implementation

The detailed information of the equations solved for the whole system was explained in the previous work of Castro et al. (2020). The model was based on heat, mass and momentum balances in each component of the system, calculating heat and mass transfer coefficients by embedding available empirical information. These equations were implemented in an in-house C++ numerical platform(NEST). For example, the control equations for the absorber are showed as

below :

$$\dot{m}_{\mathrm{s,in}} - \dot{m}_{\mathrm{s,out}} + \dot{m}_{\mathrm{v}} = \frac{dM_{\mathrm{s}}}{dt} \tag{1}$$

Equation (1) is mass balance in the liquid solution phase.

$$\dot{m}_{\mathrm{s,in}} X_{\mathrm{s,in}} - \dot{m}_{\mathrm{s,out}} X_{\mathrm{s,out}} = M_{\mathrm{s}} \frac{dX_{\mathrm{s}}}{dt} + X_{\mathrm{s}} \frac{dM_{\mathrm{s}}}{dt} \tag{2}$$

Equation (2) is LiBr balance in liquid phase.

$$M_{\mathrm{v}} R_{\mathrm{v}} T_{\mathrm{ABS}} = p_{\mathrm{ABS}} V_{\mathrm{v}} \tag{3}$$

Equation (3) is state equation of the vapour(ideal gas is assumed).

$$V_{\mathrm{v}} = V_{\mathrm{ABS}} - M_{\mathrm{s,A}} / \rho_{\mathrm{s}} \tag{4}$$

Equation (4) is volume conservation in the absorber.

$$\begin{aligned} \dot{Q}_{\mathrm{pri,ABS}} - \dot{Q}_{\mathrm{loss,ABS}} = \dot{m}_{\mathrm{s,out}} h_{\mathrm{s,out}} - \dot{m}_{\mathrm{s,in}} h_{\mathrm{s,in}} - \\ \dot{m}_{\mathrm{v,abs}} h_{\mathrm{v,abs}} + M_{\mathrm{s}} X_{p,\mathrm{s}} \frac{dT_{\mathrm{s}}}{dt} + u_{\mathrm{s}} \frac{dM_{\mathrm{s}}}{dt} \end{aligned} \tag{5}$$

Equation (5) is energy balance in the liquid phase.

$$\dot{m}_{\mathrm{s,in}} = C_d S \sqrt{\frac{2\rho_s \left[\rho_s g (H+z)\right]}{\zeta}} \tag{6}$$

Equation (6) is momentum balance at the absorber inlet.

$$\dot{m}_{\mathrm{v,abs}} = \beta_{\mathrm{ABS}} \rho_{\mathrm{s}} A \frac{1}{2} \left(\left(X_{\mathrm{in,if}} - X_{\mathrm{in,b}}\right) - \left(X_{\mathrm{out,if}} - X_{\mathrm{out,b}}\right) \right) \tag{7}$$

Equation (7) is is vapour mass transfer rate.

3. COMPARISON OF TWO WORKING PAIRS AT CHILLER MODE

In the previous work Castro et al. (2020), it was showed the transient results of the developed absorption chiller using LiBr solution in a 13 hours laboratory test campaign procedure, including start-up and shutdown. In this work, a similar test campaign procedure is carried out for the working pairs LiBr-H_2O and Carrol-H_2O, and the results are shown in Figure 3. The simulation is carried out employing PID controlled auxiliary vessels and the parameters of the controller are calculated according to Ziegler et al. (1942). Fixed temperatures in the generator secondary circuit are set as 75, 80, 85, 90, 95 are set. Each temperature will last two hours, and a warm-up for 2 hours, a shutdown of 1 hour, hence the total test campaign will be 13 hours. The results demonstrate the evolution of *COP*, cooling capacity, operation conditions, and crystallization risk against time. The crystallization risk is described as saturation rate of the solution at absorber inlet, shown as equation (8):

$$Sr_{\mathrm{in,ABS}} = X_{\mathrm{in,ABS}} / f_{\mathrm{eq}}\left(T_{\mathrm{in,ABS}}\right) \tag{8}$$

where the $Sr_{\mathrm{in,ABS}}$ is the solution saturation rate at the absorber inlet, $X_{\mathrm{in,ABS}}$ is the corresponding solution concentration at the inlet of absorber, and $f_{\mathrm{eq}}\left(T_{\mathrm{in,ABS}}\right)$ is the equilibrium concentration at corresponding temperature, when $Sr_{\mathrm{in,ABS}} > 1$ the solution will encounter crystallization risk. The results show that at chiller mode the Carrol solution has a smaller cooling capacity, a similar *COP*, and a smaller crystallization risk when compared with the LiBr solution. The cooling capacity increases with heat source temperature and decreases while ambient temperature increases, in general, these two working pairs have similar evolution characteristics. The temperatures evolution of the secondary circuit are also

demonstrated in the results, the simulations are carried out in two different T_{AMB} (ambient temperature), 30°C and 35°C. Moreover, as EG will be added to avoid the freezing problem in the heat pump mode, simulations of chiller mode with EG in the evaporator may also be interesting since this could avoid changing the liquid in the evaporator. A simulation at chiller mode with 10wt% EG added in the evaporator at T_{AMB}=35°C is carried out, as showed in picture 3. The results show the addition EG significantly decreases *COP* and cooling capacity since the EG solution has a much higher viscosity and significantly decreases the vapor pressure in the evaporator which results in a smaller mass transfer in the evaporator, as a result, the average *COP* decreases around 10% and cooling capacity decreases around 20%.

4. CARROL-H_2O WORKING PAIR AT HEAT PUMP MODE

In the heat pump mode, similar test campaigns are carried out with the working pair Carrol-H_2O, and EG is added to the evaporator to avoid the freezing problem. The test time in the test campaign at each temperature is set as 2 hours for better convergence. Figure 4 shows the numerical results of the test campaign, and in this test, the evaporator secondary circuit is considered operated under ambient condition, hence the evaporator secondary circuit inlet temperature is around ambient temperature. The indoor temperature is set as 20°C, the ambient temperature is set as 0°C, and -5°C as representative winter temperature for Barcelona and Madrid, respectively. The results demonstrate that at a lower chilled water inlet, at the heat pump mode, both *COP* and heating capacity decreases, and the crystallization risk increases. Since the heat capacity of the absorption heat pump is the sum of heat rejected from condenser and absorber (Q_{CON}+Q_{ABS}), the evolution along with time is not very sensitive to the heat source temperature, the absorption pump has an optimum performance at 75-80°C in term of *COP* and heating capacity.

5. SIMULATIONS OF 5 DAYS OF INTEGRATED SOLAR-ASSISTED ABSORPTION SYSTEM

The simulations of the absorption system with a long operation time, 5 days, are carried out to investigate the dynamic performance for a long period. In the simulations, the solar collectors are connected with the absorption system, thus a more complex control strategy is used to control the on/off of the heat source. The main purpose is to maintain the temperature of the heat tank within a range, in both modes, the heat source temperature range will be 75-90°C. When the hot water that leaves the solar collector is cooler than the water in the heat tank, the auxiliary heater will be turned on and the solar collector circuit will be closed. Hence, several parameters are used to describe the system performance. COP_{Th} is the average thermal *COP* of the machine in a day, which means the proportion of working capacity generated from the heat energy consumed, as shown in (equation 9):

$$COP_{Th} = \overline{Q}/\overline{Q}_{GEN} \tag{9}$$

Where $\overline{Q}$ is the corresponing working capacity, in chiller mode equal to $\overline{Q}_{EVA}$, while in heat pump mode equal to ($\overline{Q}_{CON} + \overline{Q}_{ABS}$).
The efficiency of the solar collector employed in the simulations is defined as below:

$$\eta_{col} = a0 - a1\frac{T_{in} - T_{AMB}}{Q_{rad}} - a2\frac{(T_{in} - T_{AMB})^2}{Q_{rad}} \tag{10}$$

Where η_{col} represents the solar collector efficiency, T_{in} is the inlet temperature in the collector, T_{AMB} is the ambient temperature, and Q_{rad} is the solar radiation. The $a0, a1, a2$ are parameters with values 0.803, 2.4, and 0.0058, respectively. The collector is a type of *High performance flat plate solar collector* (2011).

f_{solar} represents the fraction of solar energy in the total energy consumed in the absorption system, as shown in (equation 11):

$$f_{solar} = E_{col}/(E_{heat} + E_{col}) \tag{11}$$

Where E_{col} is the energy provided from the solar collectors, E_{heat} is the electricity consumption of the heater.
Table 1 shows the numerical results of the absorption system with working pairs Carrol-H_2O of 5 days in summer and winter, the $\overline{T}_{AMB}$ is the average outdoor temperature extracted from meteorologic data from Barcelona and Madrid. The data in winter is from Jan 5th to Jan 9th and in summer is from July 5th to July 9th. Moreover, 30 m^2 flat solar collectors are integrated with the hot tank as heat source, the volume of the hot tank and cold tank is 1.2 m^3, in winter the cold tank is considered been operated under atmospheric condition. The results show the average working capacity

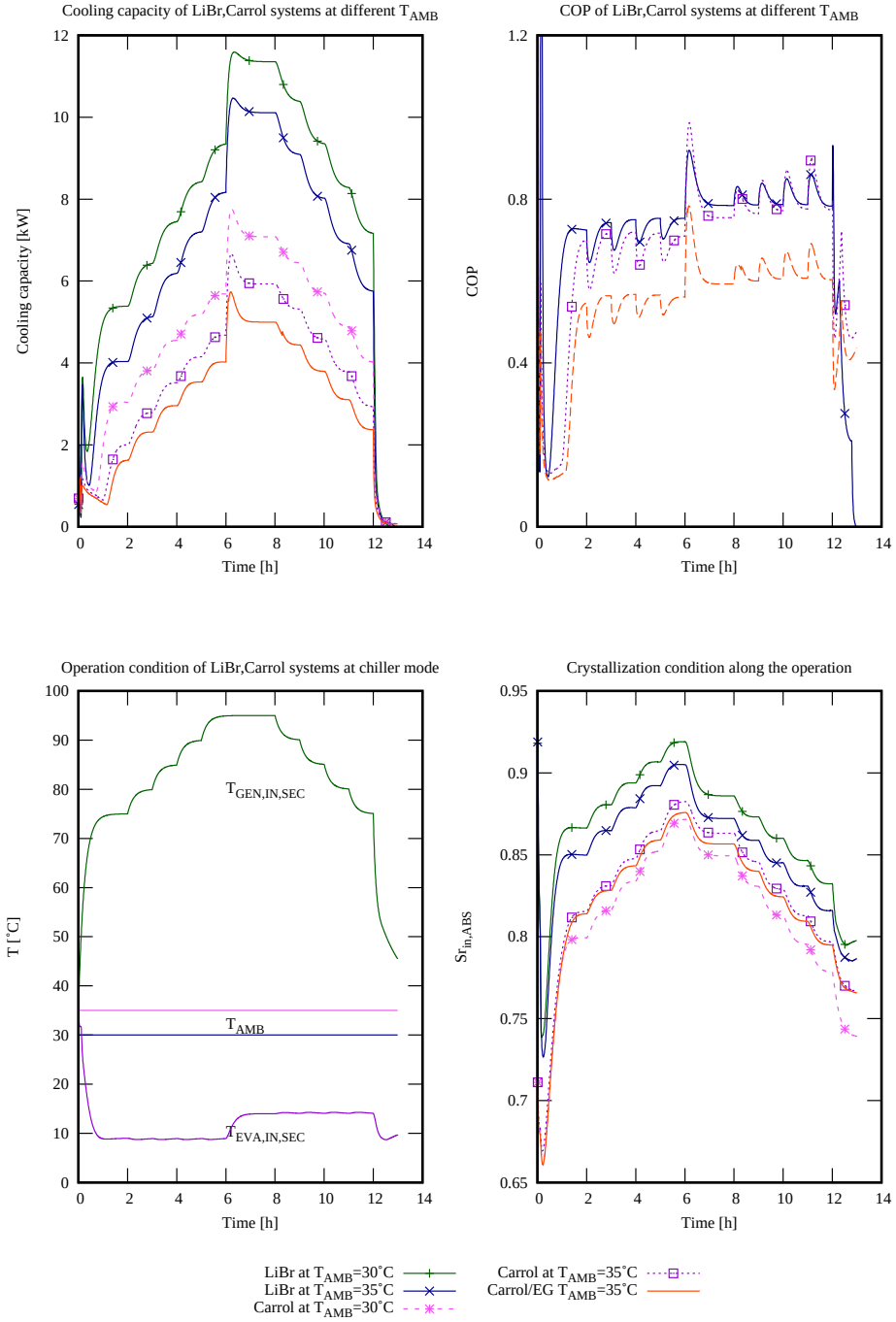

Figure 3: Absorption system numerical results at chiller application with two working pairs LiBr-H_2O and Carrol-H_2O, in which ($T_{GEN,IN,SEC}$ is the generator secondary circuit inlet temperature, (T_{AMB} is the ambient temperature, ($Sr_{in,ABS}$ is the solution saturation rate at absorber inlet, in the figure of COP, due to the similarity of the values, only results at (T_{AMB}=35°C) are demonstrated for better visualization

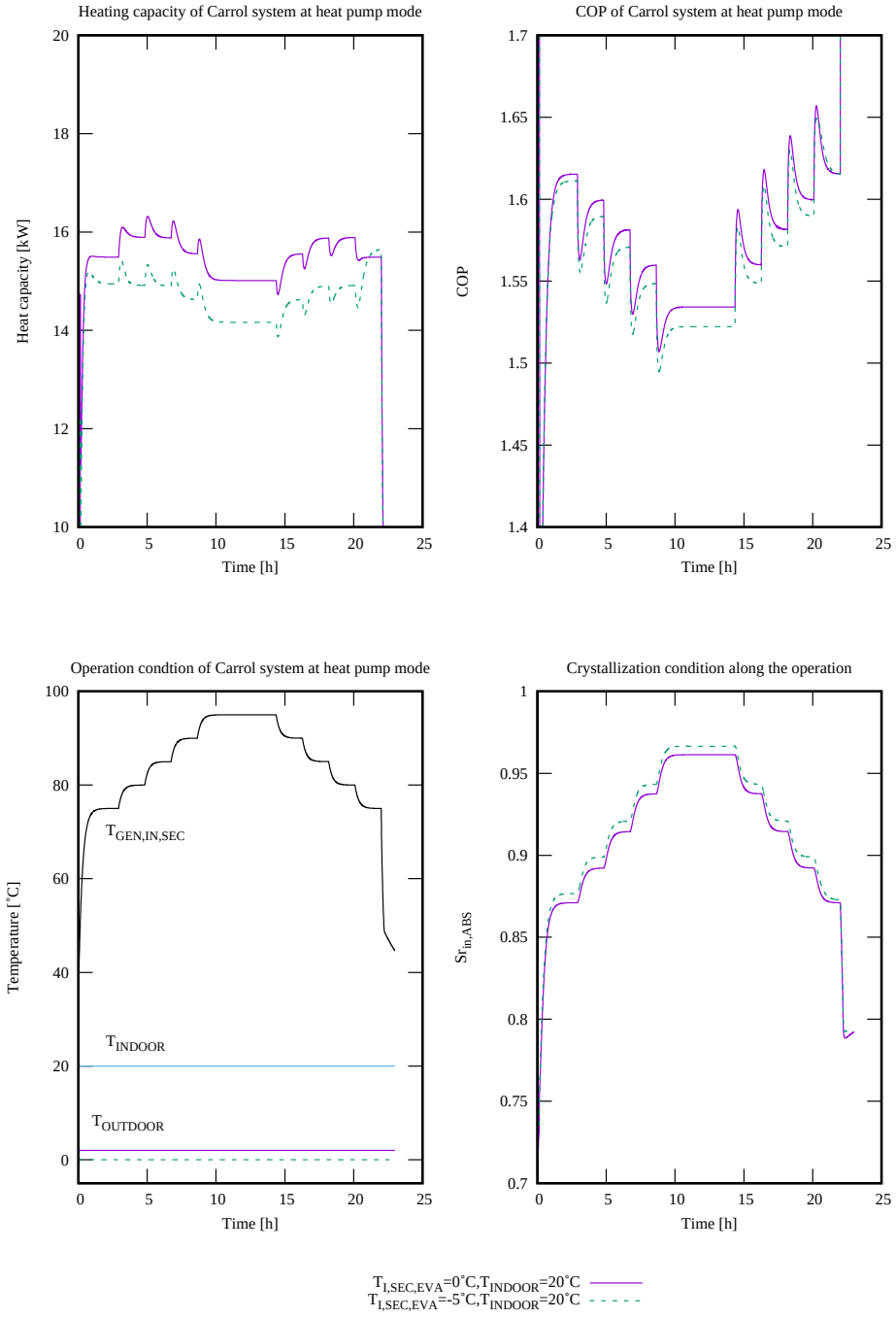

Figure 4: Absorption system at heat pump application, in which ($T_{GEN,IN,SEC}$) is the generator secondary circuit inlet temperature, (T_{INDOOR}) is the inside temperature of the residential building and ($T_{OUTDOOR}$) is the outside ambient temperature

Table 1: Numerical results of dynamic simulations of absorption system at both modes with working pair Carrol-H_2O

	Time	$\overline{T}_{AMB}$ [°C]	$\overline{Q}$ [kW]	COP_{Th}	f_{solar}
Madrid Chiller Mode	Day 1	25.5	3.9	0.74	0.40
	Day 2	26.5	3.2	0.77	0.41
	Day 3	21.3	4.1	0.80	0.62
	Day 4	20.3	4.4	0.81	0.63
	Day 5	25.1	3.6	0.78	0.62
Barcelona Chiller mode	Day 1	23.2	4.2	0.76	0.58
	Day 2	22.8	4.3	0.80	0.59
	Day 3	24.1	4.2	0.80	0.51
	Day 4	25.1	3.9	0.78	0.58
	Day 5	25.1	4.0	0.78	0.58
Madrid heat pump Mode	Day 1	3.1	14.1	1.60	0.41
	Day 2	0.0	14.7	1.61	0.48
	Day 3	0.6	15.3	1.60	0.05
	Day 4	5.2	16.2	1.61	0.12
	Day 5	6.9	15.3	1.62	0.35
Barcelona heat pump Mode	Day 1	13.9	19.9	1.65	0.002
	Day 2	13.1	19.6	1.65	0.06
	Day 3	12.3	19.2	1.65	0.06
	Day 4	10.9	18.6	1.64	0.05
	Day 5	10.4	18.4	1.64	0.02

in the corresponding days, which is around 4 kW in summer in both cities. Meanwhile in winter, the heat capacity is around 15 kW, 19 kW in Madrid, Barcelona, respectively, the heat capacity is higher in Barcelona due to the higher ambient temperature. The average COP_{Th} in chiller mode is around 0.78, and in heat pump mode is 1.62. In summer, solar energy contributes 40% - 65% of the total energy consumption, while in winter, depends on the solar radiation, the solar energy may attribute less than 5% of the total energy. There is no crystallization or freezing risk in the whole working period, which grants the advantage of the direct air-cooled integrated absorption system in both cooling and heating applications.

6. CONCLUSIONS

In this work, dynamic simulations for the absorption system at different working modes with two working pairs are presented. The results show that the working pair Carrol-H_2O has a lower cooling capacity, lower crystallization risk, and a similar *COP* when compared with LiBr solution at chiller mode. While in the heat pump mode, simulations of working pair Carrol-H_2O are carried out, the heating capacity will not be affected much by the heat source temperature, and *COP* decreases along with the heat source temperature. Also, lower evaporator secondary inlet temperature leads to lower *COP*, lower heat capacity and higher crystallization risk, moreover, the absorption system need more time to reach steady-steate in heat pump mode. The simulation results of the integrated absorption system demonstrate that on a sunny day the solar-heated water could fulfill 40-65% of total energy consumption in the climatization system, and average COP_{TH} at chiller mode is 0.73-0.81, at heat pump mode is 1.6.

NOMENCLATURE

GEN	Generator	(–)
ABS	Absorber	(–)
CON	Condenser	(–)
EVA	Evaporator	(–)
SHX	Solution heat exchanger	(–)
T	Temperature	(°C)
X	Concentration	(–)
Sr	Saturation rate of solution	(–)
COP	Coefficient of performance	(–)
C_d	Discharge coefficient	(–)
H	Height between components	(–)
z	Liquid level in component	(–)
$\dot{m}$	Mass flow rate	$(kg{\cdot}s^{-1})$
R	Specific gas constant	$(J{\cdot}kg^{-1} \cdot K^{-1})$
V	Volume	(m^3)
ρ	Density	$(kg \cdot m^{-3})$
t	Time	(s)
p	Pressure	(Pa)
S	Pipe section between components	(m^2)
$\dot{Q}$	Heat flux	(W)
ζ	Pressure loss coefficient	(–)
β	Mass transfer coefficient	(–)
η	Efficiency	(–)

Subscript

sys	system
in	inlet
out	outlet
if	interface
b	bulk
pri	primary circuit
sec	secdonary circuit
AMB	ambient
el	electricity
aux	auxiliary
th	thermal
rad	radiation
col	collector
s	solution
v	vapour

REFERENCES

Castro, J., Farnós, J., Papakokkinos, G., Zheng, J., & Oliet, C. (2020). Transient model for the development of an air-cooled libr-h2o absorption chiller based on heat and mass transfer empirical correlations. *International Journal of Refrigeration*, *120*, 406–419.

Castro, J., Oliva, A., Pérez-Segarra, C. D., & Cadafalch, J. (2007). Evaluation of a small capacity, hot water driven, air-cooled H2O-LiBr absorption machine. *HVAC and R Research*, *13*(1), 59–75. doi: 10.1080/10789669.2007.10390944

Cheng, C. S., & Shih, Y. S. (1988). Exergy and energy analyses of absorption heat pumps. *International Journal of Energy Research*, *12*(2), 189–203. doi: 10.1002/er.4440120202

Evola, G., Le Pierrès, N., Boudehenn, F., & Papillon, P. (2013). Proposal and validation of a model for the dynamic simulation of a solar-assisted single-stage LiBr/water absorption chiller. *International Journal of Refrigeration*, *36*(3), 1015–1028. doi: 10.1016/j.ijrefrig.2012.10.013

Farnós, J., Papakokkinos, G., Castro, J., Morales, S., & Oliva, A. (2017). Dynamic modeling of an air-cooled LiBr-H 2 O absorption chiller based on heat and mass transfer empirical correlations. *12th IEA Heat Pump Conference*.

Florides, G. A., Kalogirou, S. A., Tassou, S. A., & Wrobel, L. C. (2003). Design and construction of a LiBr-water absorption machine. *Energy Conversion and Management*, *44*(15), 2483–2508. doi: 10.1016/S0196-8904(03)00006 -2

Fu, D. G., Poncia, G., & Lu, Z. (2006). Implementation of an object-oriented dynamic modeling library for absorption refrigeration systems. *Applied Thermal Engineering*, *26*(2-3), 217–225. doi: 10.1016/j.applthermaleng.2005.05 .008

High performance flat plate solar collector. (2011). Retrieved from `http://www.tigisolar.com/assets/files/HoneycombCollectorwhitepaperOct11(1).pdf`

Iranmanesh, A., & Mehrabian, M. A. (2013). Dynamic simulation of a single-effect LiBr-H2O absorption refrigeration cycle considering the effects of thermal masses. *Energy and Buildings*, *60*, 47–59. doi: 10.1016/j.enbuild.2012.12 .015

Izquierdo, M., & Aroca, S. (1990). Lithium bromide high-temperature absorption heat pump: Coefficient of performance and exergetic efficiency. *International Journal of Energy Research*, *14*(3), 281–291. doi: 10.1002/er.4440140304

Jeong, S., Kang, B. H., & Karng, S. W. (1998). Dynamic simulation of an absorption heat pump for recovering low grade waste heat. *Applied Thermal Engineering*, *18*(1-2), 1–12. doi: 10.1016/s1359-4311(97)00040-9

Joudi, K. A., & Lafta, A. H. (2001). Simulation of a simple absorption refrigeration system. *Energy Conversion and Management*, *42*(13), 1575–1605. doi: 10.1016/S0196-8904(00)00155-2

Koehler, W. J., & Ibele, W. E. (1988). Availability simulation of a lithium bromide absorption heat pump. , *8*(2), 157–171.

Lee, S. F., & Sherif, S. A. (2001). Thermodynamic analysis of a lithium bromide/water absorption system for cooling and heating applications. *International Journal of Energy Research*, *25*(11), 1019–1031. doi: 10.1002/er.738

R. Reimann. (1979). *Properties of the Carrol system and a machine design for solar powered, air cooled, absorption space cooling* (Vol. 91; Tech. Rep.).

Şencan, A., Yakut, K. A., & Kalogirou, S. A. (2005). Exergy analysis of lithium bromide/water absorption systems. *Renewable energy*, *30*(5), 645–657. doi: 10.1016/j.renene.2004.07.006

Stepanov, K. I., Mukhin, D. G., Alekseenko, S. V., & Volkova, O. V. (2015). Experimental study of negative temperatures in lithium-bromide absorption refrigerating machines. *Thermophysics and Aeromechanics*, *22*(4), 481–489. doi: 10.1134/S0869864315040095

Sun, J., Fu, L., Zhang, S., & Hou, W. (2010). A mathematical model with experiments of single effect absorption heat pump using LiBr-H2O. *Applied Thermal Engineering*, *30*(17-18), 2753–2762. doi: 10.1016/j.applthermaleng.2010 .07.032

Xu, Y.-j., Zhang, S.-j., & Xiao, Y.-h. (2016). Modeling the dynamic simulation and control of a single effect libr–h2o absorption chiller. *Applied Thermal Engineering*, *107*, 1183–1191. doi: 10.1016/j.applthermaleng.2016.06.043

Ziegler, J. G., Nichols, N. B., et al. (1942). Optimum settings for automatic controllers. *trans. ASME*, *64*(11).

Zinet, M., Rulliere, R., & Haberschill, P. (2012). A numerical model for the dynamic simulation of a recirculation single-effect absorption chiller. *Energy Conversion and Management*, *62*, 51–63. doi: 10.1016/j.enconman.2012 .04.007

ACKNOWLEDGEMENT

J. Zheng holds a China Scholarship Council Studentship with the Polytechnical University of Catalonia.
Carles Oliet, as a Serra Húnter lecturer, acknowledges the Catalan Government for the support through this Programme.